Hygrothermoelastic Analysis of Orthotropic Cylindrical Shells

Abstract

In this work, the combined effect of moisture and temperature on the bending behavior of simply supported orthotropic cylindrical shells has been investigated. Initially three dimensional equilibrium equations of thermoelasticity, simplified to the case of generalized plane strain deformations in the axial direction are solved analytically for an orthotropic cylindrical shell strip under thermal loading. Based on the realistic variation of displacements from the elasticity approach, a new higher order shear deformation theory was proposed for the analysis of an orthotropic cylindrical shell strip under hygrothermal and mechanical loading. The zigzag form of the displacement is incorporated via the Murakami zigzag function. Results are presented for mechanical and thermal loading for various layups and they are validated against the derived elasticity solution. The significance of retaining various higher-order terms in the present model, in evaluating the stresses and deflection for composite laminates is brought out clearly through parametric study. Useful results for combined hygrothermal loading are presented in tabular and graphical form. It is expected that the numerical results presented herein will serve as bench mark in future.

J.S.Mohamed Ali [a]
Saleh Alsubari [b]
Yulfian Aminanda [c]

[a,b,c] International Islamic University Malaysia (IIUM), Malaysia.
[a] jaffar@iium.edu.my
[b] snsubari@gmail.com
[c] yulfian@iium.edu.my

1 INTRODUCTION

Applications of the laminated composite structures have been increasing in the field of aerospace, automobile, civil and other engineering, as these structures possess advantages of high specific stiffness and high specific strength with a good tailoring capability. Aerospace structures such as wings or fuselages are mostly assemblies of shell structures, these structures are exposed to environmental conditions such as high temperature and moisture effect that are detrimental to the strength and stiffness of the composite structures. Hence the analysis of such composite shell structures under hygrothermal loading has been of considerable interest to researchers.

Classical shell theories originally developed for analysis of thin elastic shells based on the Love-Kirchhoff assumptions are not applicable for the analysis of laminated composite shells, as these theories neglect the effect of transverse shear deformations. Thus the application of such theories to laminated composite shells where shear deformation is very significant, such as thick laminates, may lead to errors in calculating deflections and stresses. Whereas higher order theories which account for shear deformation are useful to accurately model such laminated composite shells.

In order to establish the accuracy of any shell theory, it is important to compare the results with the benchmark results based on theory of elasticity, because they represent closer approximation to actual behavior of the structure than the commonly used engineering theories of bending. Thus such a solution can be deemed as a standard benchmark for determining the range of applicability of classical as well as other engineering theories. This has been the prime motivation for three dimensional analyses of beam, plate and shell structures. Such elasticity solutions are limited only for specific geometry and boundary conditions; hence one has to resort to approximate classical and higher order theories for complex loading and geometry.

Considerable work on the analysis of laminated composite shells has been reported by Noor et al. (1991) and Noor and Burton (1992). Other notable work on laminated shells under thermal/hygrothermal loading based on theory of elasticity/higher order models are as follows.

Huang and Tauchert (1991)&(1992) have presented elasticity solutions for cross-ply cylindrical panels and doubly curved cross-ply laminates. Burton and Noor (1994) presented three-dimensional thermoelasticity solutions for sandwich panels and cylindrical shells subjected to thermo- mechanical loads. Khdier (1996) presented thermoelastic analysis of cross-ply circular cylindrical shells using the higher order theory of JN Reddy. Ding and Tang (1998) have derived exact thermoelastic solution for an axisymmetric problem of thick closed laminated shells while Xia and Ding (2001) derived a three-dimensional thermoelastic solution for laminated cantilever cylindrical shell. Khare et al.(2003) presented closed-form solution of 2D higher-order shear deformation theories for the thermo-mechanical analysis of simply supported doubly curved cross-ply laminated shells. In addition, Sayman Onur (2005) presented the stress analysis of thick multi-layered composite cylindrical shells under hygrothermal loading using elasticity solutions based on the Lekhnitskii's theory for plane strain case.

Furthermore, Naidu and Sinha (2005) presented a finite element formulation based on FSDT for large deformation behavior of laminated composite cylindrical shell panels subjected to hygrothermal environments. Jacob and Senthil (2006) derived an exact solution for thermoelastic response of functionally graded orthotropic cylindrical shells. In another study, Brischetto and Carrera (2008) study the thermal stress analysis of composite shell by refined multilayered models. A study on the free-edge effects in laminated circular cylindrical shell panels subjected to hygrothermal loading is carried out by Nosier and Miri (2009) by utilizing displacement-based theories. A complete review on the analysis of laminated composite shells under thermal and hygrothermal loading from 2000 to 2010 has been recently reported by Qatu et al. (2012). Yifeng and Yu (2011) constructed a hygrothermoelastic model capable of performing a hygrothermoelastic stress analysis of composite laminates by using variational-asymptotic method. Later on, Lal et al. (2011) investigated the effect of random system properties on transverse nonlinear central deflection of laminated composite spherical shell panel subjected to hygro-thermo-mechanical loading using higher order

theory proposed by JN Reddy. Brischetto and Carrera (2012) studied the static analysis of multi-layered smart shells subjected to mechanical, thermal and electrical loads by using Carrera Unified Formulation (CUF).

Recently in 2013, Jafari et al. (2013) presented the thermo-elastic response of a 2-D functionally graded open cylindrical shell with temperature-dependent material properties based on third-order shear deformation plate theory of JN Reddy.

Very recently, Brischetto (2013) analyzed multilayered composite and sandwich shells under hygrothermal loads using refined two-dimensional models that has been developed based on Carrera Unified Formulation (CUF).

A careful study of the references on thermally loaded laminated shells based on elasticity reveals that most of them provide just the solutions but not useful numerical results in the form of deflections and stresses for various span to thickness ratio as has been reported by Pagano(1970b)&(1970a) for laminated plates under mechanical loading, Ren (1987), Bhaskar and Varadan (1993) for laminated shells under mechanical loading and Bhaskar et al. (1996) for plates under thermal loading. Taking care to note, that, these works has formed a well-established basis for assessment, as well as development of the methodology for various laminate theories and is most commonly referred to, one can recognize the absence of such important benchmark results for the flexure of thermally loaded orthotropic laminated shells. Thus the objective of this present study is to present benchmark results in a form suitable for the evaluation of various shell theories for orthotropic laminated shells under thermal loading. Having derived the benchmark results, then from the realistic variations of displacements based on the elasticity approach were used to develop an accurate higher order model for analysis of laminates under hygrothermal loading.

2 FORMULATION

2.1 Elasticity Solution

A N-layered cylindrical shell strip that is infinitely long in the axial direction as shown Fig. 1 is considered. The fiber orientation of any layer is either parallel along θ or z direction. The equations governing the cylindrical bending of the shell are:

2.1.1 Equilibrium Equations

$$\sigma_{r,r} + \frac{\tau_{r\theta,\theta}}{r} + (\sigma_r - \sigma_\theta)/\mathrm{r} = 0$$
$$\tau_{r\theta,r} + \frac{\sigma_{\theta,\theta}}{r} + 2\tau_{r\theta}/r = 0$$

$$(1)$$

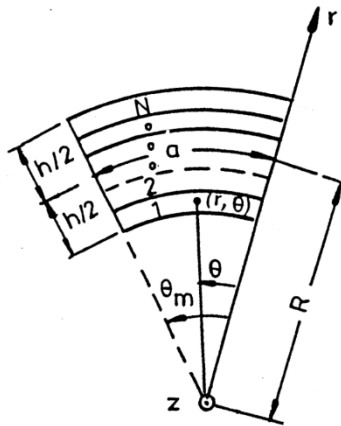where a subscript comma denotes differentiation.

Figure 1: Geometry and coordinate system of shell

2.1.2 Thermoelastic Stress-Strain Law

$$\begin{Bmatrix} \sigma_r \\ \sigma_\theta \\ \sigma_z \\ \tau_{\theta z} \end{Bmatrix} = \begin{bmatrix} C_{11} & C_{12} & C_{13} & 0 \\ C_{12} & C_{22} & C_{23} & 0 \\ C_{13} & C_{23} & C_{33} & 0 \\ 0 & 0 & 0 & C_{44} \end{bmatrix} \begin{Bmatrix} \varepsilon_r - \alpha_r T \\ \varepsilon_\theta - \alpha_\theta T \\ \varepsilon_z - \alpha_z T \\ \gamma_{\theta z} \end{Bmatrix} \tag{2a}$$

$$\begin{Bmatrix} \tau_{rz} \\ \tau_{r\theta} \end{Bmatrix} = \begin{bmatrix} C_{55} & 0 \\ 0 & C_{66} \end{bmatrix} \begin{Bmatrix} \gamma_{rz} \\ \gamma_{r\theta} \end{Bmatrix} \tag{2b}$$

where C_{ij}'s and α_i's are the stiffness coefficients and the coefficients of thermal expansion, respectively, transformed from the material co-ordinates to the geometric co-ordinates. $T(r,\theta)$ is the change in temperature with reference to the stress-free isothermal state.

2.1.3 Strain -Displacement Relations

$$\begin{aligned} \varepsilon_r &= u_{r,r} \\ \varepsilon_\theta &= (u_{\theta,\theta} + u_r)/r \\ \gamma_{r\theta} &= (u_{r,\theta} - u_\theta)/r + u_{\theta,r} \end{aligned} \tag{3}$$

where u_r and u_θ are the displacements in r and θ directions respectively.

Using Eqns. (2) and (3), the equilibrium equations (Eqn. (1)) can be written in terms of displacements as

$$[L]\{u\} = \{t\} \tag{4}$$

where $[L]$ and $\{t\}$ are function of C_{ij}'s and α_i's, and $\{u\}$ is the displacement vector.
The temperature variation is taken as

$$T = T_0(r)\,sin(m\,\pi\theta/\theta_m) \tag{5}$$

The longitudinal edges are assumed to be simply-supported such that

$$u_r = \sigma_\theta = 0 \ \text{ at } \theta=0,\ \theta_m \tag{6}$$

2.1.4 Solution

A solution for Eqn. (4) satisfying the conditions of Eqn. (6), can be assumed as

$$
\begin{Bmatrix} u_r \\ u_\theta \end{Bmatrix} = \begin{Bmatrix} \emptyset_r \, sin(m\pi\theta/\theta_m) \\ \emptyset_\theta \, cos \, (m\pi\theta/\theta_m) \end{Bmatrix}
\tag{7}
$$

where ϕ_r and ϕ_θ are functions of r. Substitution of this solution in Eqn. (4) yields a set of coupled fourth order system of non-homogeneous ordinary differential equations with variable coefficients, which can be further reduced to a set of ordinary differential equations with constant coefficients by a simple transformation [Wylie and Barrett (2012)]. Thus the final solution in terms of complementary solution and particular integral results in evaluation of four arbitrary constants per layer. Thus for an N-layer laminate there will be 4N unknown constants. These can be determined by enforcing the continuity of the displacements $u_r \, and \, u_\theta$ and the transverse stresses $\tau_{r\theta}$ and σ_{rr} at the (N-1) interfaces of the laminate, along with the following lateral surface conditions

$$
\tau_{r\theta} = \sigma_{rr} = 0
\tag{8}
$$

2.2 Higher Order Model

2.2.1 Definition of Displacement Field

Based on the results from elasticity solution, it can be proposed that the following complete model with 13 terms are required to accurately predict the behavior of a finite cross-ply shell under thermal loading

$$
\begin{aligned}
u &= u_o + z\emptyset_x + z^2 \, \lambda_x + z^3 \, \zeta_x + \psi_k S_x \\
v &= v_o + z\emptyset_\theta + z^2 \, \lambda_\theta + z^3 \, \zeta_\theta + \psi_k S_\theta \\
w &= w_o + z w_1 + z^2 \, \Gamma
\end{aligned}
\tag{9}
$$

To demonstrate the capability of the proposed model, the formulation was made for the case of cylindrical bending similar to the elasticity solution with only v and w ($u_\theta \, and \, u_r$).
Consider an infinitely long laminated cylindrical shell panel. The panel coordinate system is such that $0 \leq x \leq \infty$, $0 \leq \theta \leq \theta_m$ and $-h/2 \leq z \leq h/2$. The mean radius of the shell strip is considered as R and the load is uniform along the x axis so that the shell undergoes cylindrical bending ($\varepsilon_x = 0$).

$$
\begin{aligned}
v &= v_o + z\emptyset_\theta + z^2 \, \lambda_\theta + z^3 \, \zeta_\theta + \psi_k S_\theta \\
w &= w_o + z w_1 + z^2 \, \Gamma
\end{aligned}
\tag{10}
$$

The other displacement model assumed here is HSDT6 by neglecting the higher order terms in w which is described as:

$$
\begin{aligned}
v &= v_o + z\emptyset_\theta + z^2 \, \lambda_\theta + z^3 \, \zeta_\theta + \psi_k S_\theta \\
w &= w_o
\end{aligned}
\tag{11}
$$

where v and w are the displacements at any point in the laminate. The parameter v_o is the in-plane displacement, and w_o is the transverse displacement of a point on the middle plane. The functions

ϕ_θ is the rotation of the normal to the middle plane about θ. The other parameters $\lambda_\theta, \zeta_\theta, w_1$ and Γ are unknown higher-order terms which are function of θ only. ψ_k is the zigzag function term as defined by Murakami (Murakami, 1986)

$$\psi_k = 2(-1)^k z_k / h_k \tag{12}$$

where z_k is a local transverse coordinate with its origin at the center of the kth layer and h_k is the corresponding layer thickness.

The stress-stain law for the kth layer with respect to the (x, θ) coordinate is given by:

$$\begin{Bmatrix} \sigma_x \\ \sigma_\theta \\ \sigma_z \\ \tau_{\theta z} \\ \tau_{xz} \\ \tau_{x\theta} \end{Bmatrix} = \begin{bmatrix} C_{11} & C_{12} & C_{13} & 0 & 0 & 0 \\ C_{12} & C_{22} & C_{23} & 0 & 0 & 0 \\ C_{13} & C_{23} & C_{33} & 0 & 0 & 0 \\ 0 & 0 & 0 & C_{44} & 0 & 0 \\ 0 & 0 & 0 & 0 & C_{55} & 0 \\ 0 & 0 & 0 & 0 & 0 & C_{66} \end{bmatrix}^k \begin{Bmatrix} \varepsilon_{xx} - \Delta T \alpha_x - \Delta C \beta_x \\ \varepsilon_{\theta\theta} - \Delta T \alpha_\theta - \Delta C \beta_\theta \\ \varepsilon_{zz} - \Delta T \alpha_z - \Delta C \beta_z \\ \gamma_{\theta z} \\ \gamma_{xz} \\ \gamma_{x\theta} \end{Bmatrix} \tag{13}$$

where the $C_{ij}^{k\prime}s$ are the transformed elastic coefficients and $\Delta T = T - T_0$, $\Delta C = C - C_0$, in which, $T(x, \theta, z)$ and $C(x, \theta, z)$ are the temperature and moisture loads variations through the thickness respectively, whereas T_0 and C_0 are the reference temperature and moisture concentration respectively. α_x, α_θ, and α_z are the thermal expansion coefficients and β_x, β_θ and β_z are the moisture expansion coefficients respectively.

Expression for the principle of virtual work is

$$\iiint (\sigma_x \delta\varepsilon_x + \sigma_\theta \delta\varepsilon_\theta + \sigma_z \delta\varepsilon_z + \tau_{xz} \delta\gamma_{xz} + \tau_{x\theta} \delta\gamma_{x\theta} + \tau_{\theta z} \delta\gamma_{\theta z}) dz dA - \iint q\, \delta w dA = 0 \tag{14}$$

where q is the load per unit area on the mid-surface of the shell.

Integrating the displacement gradient given in Eq. (14) for the case of cylindrical bending by parts and by setting the coefficient of $\delta v_0, \delta w_0, \delta\emptyset_\theta, \delta\lambda_\theta, \delta\zeta_\theta, \delta S_\theta, \delta w_1$ and $\delta\Gamma$ to zero separately, we obtain the following equilibrium equations with associated boundary conditions.

$$\begin{aligned} N_{\theta,\theta} + N_{\theta z} = 0; &\qquad J_{\theta,\theta}/R - J_{\theta z} = 0 \\ M_{\theta,\theta}/R - N_{\theta z} = 0; &\qquad N_{\theta z,\theta} - N_\theta + Rq = 0 \\ K_{\theta,\theta} - T_{\theta z} = 0; &\qquad M_{\theta z,\theta} - M_\theta - RN_z = 0 \\ H_{\theta,\theta} - H_{\theta z} = 0; &\qquad K_{\theta z} - K_\theta - 2RM_z = 0 \end{aligned} \tag{15}$$

The equilibrium equations for displacement models HSDT6 are the first six equations of displacement model HSDT8 given in Eq. (15)

Boundary conditions are given as

At $\theta = 0$ constant: one from each of the following bracketed quantities should be specified:

$$\begin{aligned} &(N_\theta, v_0), (M_\theta, \phi_\theta), (K_\theta, \lambda_\theta), (J_\theta, \zeta_\theta), \\ &(H_\theta, S_\theta), (N_{\theta z}, w_0), (M_{\theta z}, w_1) \text{ and } (K_{\theta z}, \Gamma) \end{aligned} \tag{16}$$

The generalized stress resultants occurring in Eq. (15) are defined as follows:

$$(N_\theta, M_\theta, K_\theta, J_\theta, H_\theta) = \sum_{k=1}^{N} \int \sigma_\theta^{(k)} \left(1, z, z^2, z^3, \psi_k\right) dz^{(k)}$$

$$(N_z, M_z) = \sum_{k=1}^{N} \int \sigma_z^{(k)} \left(1 + \frac{z}{R}\right)(1, z) dz^{(k)}$$

$$\begin{aligned} &(N_{\theta z}, M_{\theta z}, K_{\theta z}, H_{\theta z}, J_{\theta z}, T_{\theta z}) = \\ &\sum_{K=1}^{N} \int \tau_{\theta z}^{(k)} \left(1, z, z^2, \frac{2(-1)^k(R+z)}{h_k}, (3Rz^2 - 2z^3), (3Rz - 2z^2)\right) dz^{(k)} \end{aligned}$$

(17)

The integration being from $-h_k/2$ to $h_k/2$ and the summation being carried out over the N of shells.

From Eqns. (10-13), the stress resultants can be expressed in terms of displacements, hence the equilibrium equations can be written in terms of generalized displacements in operator form as:

$$[L]\{\delta\} = \{f\} \tag{18}$$

where [L] is a matrix of differential operators with respect to θ, $\{\delta\}$ represent the displacement vector [v_0 ϕ_θ λ_θ ζ_θ S_θ w_0 w_1 Γ] and $\{f\}$ is the load vector that depends on the mechanical and hygrothermal load.

The solution assumed for Eq. (18) expressed in terms of displacements which satisfies the above boundary conditions Eq. (16) is:

$$\begin{aligned} (v_0, \phi_\theta, \lambda_\theta, \zeta_\theta, S_\theta) &= (P_1, P_2, P_3, P_4, P_5) \cos(\pi\theta/\theta_m) \\ (w_0, w_1, \Gamma) &= (P_6, P_7, P_8) \sin(\pi\theta/\theta_m) \end{aligned} \tag{19}$$

where P_1 to P_8 are the displacement amplitudes. Using Eq. (19) in Eq. (18) results in a system of linear algebraic equations and by solving these equations, unknown coefficient $\{\delta\}$ can be obtained readily and subsequently in-plane stresses and transverse stresses can be obtained. Although the transverse shear stresses can be calculated from the constitutive relations, these stresses may not satisfy the continuity conditions at the interface between layers, hence transverse shear stresses are obtained by integrating three dimensional equilibrium equations of elasticity.

3 RESULTS AND DISCUSSION

In this section, initially, benchmark results based on elasticity are generated for cylindrical shell strips under mechanical loading to validate the analytical formulation of both the elasticity approach and the new higher order model developed.   Then the results are presented for both mechanical and hygrothermal loads for various cross-ply layups and through the thickness variations of displacements and stresses are given for various R/h ratios.

All laminas are assumed to be of the same thickness and made of the same orthotropic materials with the following lamina properties (Bhaskar et al. (1996)).

$$\frac{E_L}{E_T} = 25; \frac{G_{LT}}{E_T} = 0.5 \; ; \frac{G_{TT}}{E_T} = 0.2; \; v_{LT} = v_{TT} = 0.25 \text{ and } \frac{\alpha_T}{\alpha_L} = 1125$$

Here L and T refer to the properties parallel and perpendicular respectively to the fiber.

All the results are generated for laminates with simply supported boundary condition such that at θ=constant

$$N_\theta = M_\theta = K_\theta = J_\theta = H_\theta = w_0 = w_1 = \Gamma = 0 \tag{20}$$

All reported results for thermal and hygrothermal loads are normalized using the following dimensionless expression except that for the mechanical loading which is stated in the corresponding Table.

$$\bar{w} = w/(h\alpha_L\bar{T}_0 S^2); (\bar{v}) = (v)/(h\alpha_L\bar{T}_0 S)$$
$$(\bar{\sigma}_i, \bar{\tau}_{ij}) = (\sigma_i, \tau_{ij})/(E_T\alpha_L\bar{T}_0) \text{ , where } S=R/h \tag{21}$$

3.1 Validation of the Laminate Model

For validating the formulation of the new higher order model HSDT8 of the orthotropic laminated shell, initially the laminate is considered to be under mechanical loading for which the elasticity results are regenerated using Ren's formulation (Ren (1987)). A simply supported laminated shell made of symmetric three-layer cross-ply (90/0/90) under mechanical loading was considered. The results for both the elasticity and higher order model HSDT8 are presented in Table 1 for comparison. The results for both stresses and displacements are found to agree very well even for thick laminates (R/h=4). It should be noted that the reported values of displacements and stresses based on elasticity has been generated using the elasticity formulation derived in this paper.

R/h	Theory	$\bar{w}(0,\text{-}h/2)$	$\bar{v}(0,\text{-}h/2)$	$\bar{\sigma}_x(\pm h/2)$	$\bar{\sigma}_\theta(\pm h/2)$	$\bar{\tau}_{\theta z}(\pm h/6)$
4	HSDT8	4.0629	5.1029	0.0050	1.2111	0.4093
		4.1222	7.0811	-0.0252	-1.6598	0.4778
	Elasticity	3.9818	5.1511	0.0283	1.2752	0.4112
		4.0194	6.9449	-0.0165	-1.6441	0.4845
10	HSDT8	1.2236	3.8797	0.0054	0.8124	0.4780
		1.2266	4.9994	-0.0125	-0.9116	0.5082
	Elasticity	1.2180	3.8731	0.0107	0.8189	0.4780
		1.2205	4.9812	-0.0091	-0.9085	0.5082
20	HSDT8	0.7866	5.0021	0.0059	0.7307	0.4889
		0.7867	5.9609	-0.0093	-0.7712	0.5042
	Elasticity	0.7862	5.2657	0.0079	0.7328	0.4890
		0.7861	5.9573	-0.0077	-0.7698	0.5040
50	HSDT8	0.6595	10.4948	0.0065	0.7060	0.4907
		0.6595	11.4017	-0.0078	-0.7211	0.4967
	Elasticity	0.6595	10.4946	0.0072	0.7067	0.4907
		0.6595	11.4015	-0.0072	-0.7204	0.4966
100	HSDT8	0.6398	20.3639	0.0068	0.7026	0.4934
		0.6398	21.2610	-0.0074	-0.7100	0.4904
	Elasticity	0.6397	20.3628	0.0070	0.7028	0.4933
		0.6397	21.2594	-0.0071	-0.7096	0.4904

* z values are given in parentheses; θ values are such that the sin or cos function become a maximum

Table 1: Dimensionless maximum displacements and stresses of cross-ply (90/0/90) cylindrical shell strips subjected to mechanical loading

As there are no benchmark results available in the literature for validation of higher order models for thermal loading; firstly, benchmark results based on the developed elasticity solution are generated for simply supported laminated shell strip under thermal loading. The results are presented in Table 2-4 for laminated shells made of (a) a unidirectional shell with the fibers oriented in the θ direction (90); (b) bidirectional laminated cylindrical shell with the T and L directions parallel the θ-direction in the bottom and top layers respectively, the layers being of equal thickness (90/0); (c) a symmetric 3-ply cylindrical shell with layers of equal thickness-the L direction coincides with the ϑ-direction in the outer layers, while T is parallel to the θ-direction in the central layer (90/0/90).

For these problems the shell strip was considered to be subjected to temperature field linearly varying through the thickness (i.e.. $T = 2\overline{T}_0(z/h)\sin(m\pi\theta/\theta_m)$). For to understand the capability of the HSDT8 in predicting the stresses and displacements accurately, results based on HSDT8 are also included in Table 2 and 3 for comparison and hence the validation of this higher order model under thermal loading. The results for both stresses and displacements are found to agree well even for thick laminates (R/h= 4) for all cases as shown in the following tables.

R/h	Theory	$\overline{w}(\pm h/2)^*$	$\overline{v}(\pm h/2)$	$\overline{\sigma}_x(\pm h/2)$	$\overline{\sigma}_\theta(\pm h/2)$	$\overline{\tau}_{\theta z}(\pm h/4)$
4	HSDT8	20.4768	1.3363	-1117.50	1138.7	67.89
		20.9610	5.8297	1136.80	617.2	-65.36
	Elasticity	20.3599	1.1750	-1113.21	1178.4	57.16
		20.7900	5.5470	1131.92	692.1	-54.71
10	HSDT8	5.7233	0.6527	-1118.90	570.1	15.67
		5.7306	1.1611	1132.60	486.8	-15.55
	Elasticity	5.7026	0.6468	-1119.30	569.1	14.99
		5.7090	1.5993	1129.80	487.7	-14.87
20	HSDT8	3.5068	0.7260	-1121.50	293.2	4.18
		3.5070	1.1385	1129.00	272.7	-4.16
	Elasticity	3.5023	0.7248	-1123.83	292.2	4.11
		3.5020	1.1366	1127.71	271.8	-4.10
50	HSDT8	2.8815	0.8085	-1123.50	117.1	0.68
		2.8815	0.9659	1126.60	113.8	-0.68
	Elasticity	2.8791	0.8078	-1123.83	116.4	0.67
		2.8791	0.9655	1126.13	113.6	-0.68
100	HSDT8	2.7920	0.8421	-1124.24	58.3	0.17
		2.7920	0.9203	1125.80	57.8	-0.17
	Elasticity	2.7851	0.8400	-1124.42	58.0	0.16
		2.7851	0.9190	1125.58	57.3	-0.17

* z values are given in parentheses; θ values are such that the sin or cos function become a maximum

Table 2: Dimensionless maximum displacements and stresses of (90) cylindrical shell strips subjected to thermal loading

R/h	Theory	$\overline{w}(\pm h/2)^*$	$\overline{v}(\pm h/2)$	$\overline{\sigma}_x(\pm h/2)$	$\overline{\sigma}_\theta(0,-h/2)$	$\overline{\tau}_{\theta z}(0)$
4	HSDT8	74.09	-24.02	-156.00	2216.54	-105.85
		75.83	28.90	1112.10	-1407.10	-105.85
	Elasticity	76.93	-24.51	-169.85	2427.50	-98.93
		78.83	30.39	1109.01	-1598.95	-105.85
10	HSDT8	54.42	4.36	-202.60	2713.86	-51.29
		54.72	20.08	1103.10	-1903.01	-51.29
	Elasticity	55.04	4.42	-208.79	2756.8	-50.54
		55.34	20.32	1105.69	-1931.53	-51.30
20	HSDT8	50.48	10.33	-215.60	2813.46	-26.55
		50.56	17.55	1101.90	-2054.60	-26.55
	Elasticity	50.65	10.37	-218.62	2824.30	-26.42
		50.72	17.61	1104.40	-2059.68	-26.42
50	HSDT8	48.82	13.39	-222.01	2848.35	-10.74
		48.84	16.15	1101.80	-2130.70	10.74
	Elasticity	48.85	13.39	-222.95	2848.96	-10.72
		48.86	16.17	1103.70	-2129.71	-10.72
100	HSDT8	48.39	14.34	-223.91	2855.46	-5.38
		48.39	15.71	1101.80	-2153.00	-5.38
	Elasticity	48.39	14.34	-224.10	2853.80	-5.37
		48.39	15.71	1103.50	-2150.91	-5.37

* z values are given in parentheses; θ values are such that the sin or cos function become a maximum.

Table 3: Dimensionless maximum displacements and stresses of cross-ply (90/0) cylindrical shell strips subjected to thermal loading

R/h	Theory	$\overline{w}(\pm h/2)^*$	$\overline{v}(\pm h/2)$	$\overline{\sigma}_x(\pm h/2)$	$\overline{\sigma}_\theta(\pm h/6)$	$\overline{\tau}_{\theta z}(\pm h/6)$
4	HSDT8	19.64	1.32	-1115.3	-398.6	9.62
		19.80	5.50	1136.2	347.2	2.06
	Elasticity	19.60	1.92	-1131.3	-396.9	10.12
		19.75	5.39	1114.1	347.3	2.21
10	HSDT8	5.87	0.78	-1119.0	-384.3	3.62
		5.86	1.80	1130.9	359.3	2.20
	Elasticity	5.86	0.78	-1119.9	-383.6	3.71
		5.85	1.80	1128.6	359.3	2.21
20	HSDT8	3.83	0.84	-1121.5	-378.0	1.66
		3.83	1.30	1127.8	365.1	1.29
	Elasticity	3.83	0.84	-1122.2	-377.7	1.69
		3.83	1.30	1126.7	365.1	1.30
50	HSDT8	3.25	0.92	-1123.3	-374.0	0.63
		3.25	1.10	1125.9	368.9	0.57
	Elasticity	3.25	0.92	1123.6	-373.9	0.62
		3.25	1.10	1125.5	368.8	0.56
100	HSDT8	3.17	0.96	-1123.9	-372.7	0.30
		3.17	1.04	1125.2	370.2	0.29
	Elasticity	3.17	0.95	-1124.1	-372.6	0.30
		3.17	1.04	1125.1	370.1	0.29

* z values are given in parentheses; θ values are such that the sin or cos function become a maximum

Table 4: Dimensionless maximum displacements and stresses of cross-ply (90/0/90) cylindrical shell strips subjected to thermal loading

Through the thickness variations of the displacements and stresses in the (90/0/90) shell strip presented in Figs 2 and 3. As can be seen from Fig.2, the variation of $\overline{w}$ is small for R/h=10. for a thick laminate with R/h=4, $\overline{w}$ varies significantly, thus while developing refined theories for thermal stress analysis of thick laminates, it is necessary to account for the thickness-stretch effect. Based on this observation from elasticity results, higher order terms have been considered for w in the higher order model (HSDT8). The variation of the in-plane displacement for thermal loading are shown in Fig 3, from which it can be noted that there is a considerable warping of the normal and a pronounced zig-zag effect for the case of the thick laminates. To show the importance of zig-zag term in the developed HSDT8 on the accurate prediction of in-plane displacement, through the thickness variation of inplane displacement with (HSDT8) and without zig zag term (HSDTWZ) in the Higher order model for both thermal and mechanical loading are graphed in Fig 4 and Fig 5 respectively. It can be noted from theses figures that zig-zag term is important in v for accurate prediction of displacements.
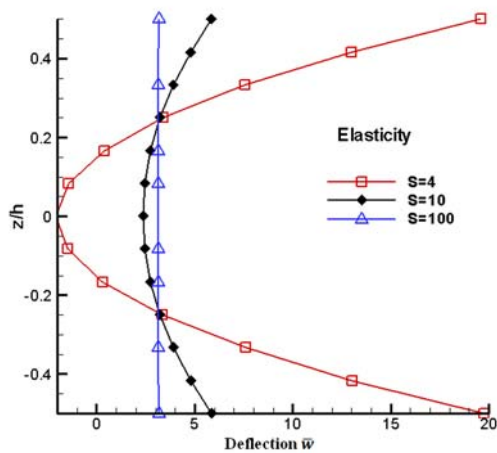
Figure 2: Varaition of deflection $\overline{w}$ under thermal loading for (90/0/90) shell strip
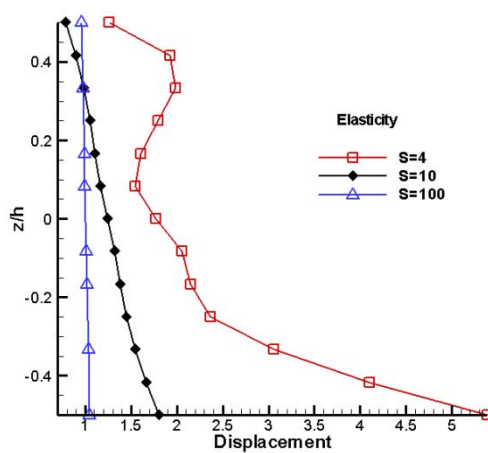
Figure 3: Varaition of displacement $\overline{v}$ under thermal loading for (90/0/90) shell strip

To show the importance of the zig-zag function and the thickness stretch/contraction term, results obtained by dropping these terms from HSDT8 are also included in Figs 4-9 and Table 5. The thickness wise variations of the deflection, in-plane stresses and interlaminar stresses $\overline{\tau}_{\theta z}$ are given in Figs 6-9 for (90/0/90) cylindrical shell strip under thermal loading. From the above Tables and Figures it can be seen that not only the displacements but also the in-plane and the interlaminar stresses are accurate even for thick laminates under thermal loading. In all the above Tables, results and graphs for $\overline{\sigma}_r$ (or $\overline{\sigma}_z$) have not been presented. It is expected that once the transverse shear stresses are estimated accurately, their use with the integration of three-dimensional equilibrium equation would automatically yield accurate values of $\overline{\sigma}_r$ (or $\overline{\sigma}_z$).
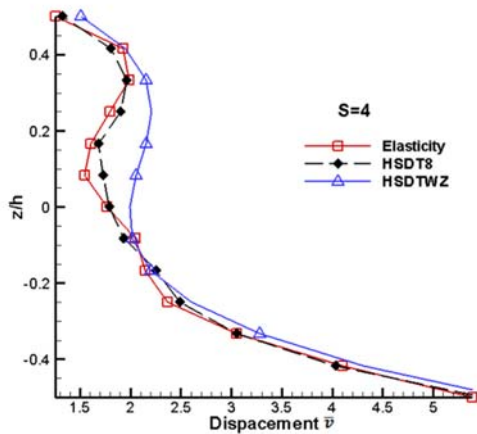
Figure 4: Varaition of displacement $\overline{\nu}$ under thermal loading for (90/0/90) shell strip
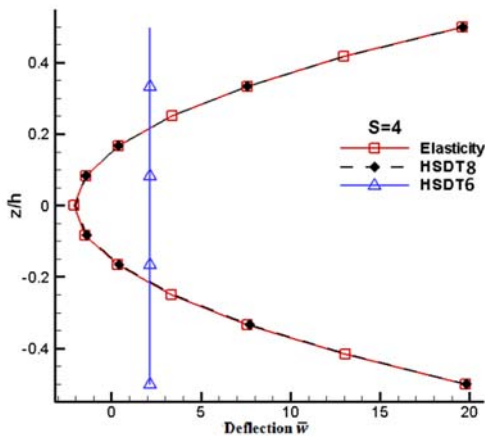

Figure 5: Varaition of displacement $\overline{\nu}$ under mechanical loading for (90/0/90) shell strip

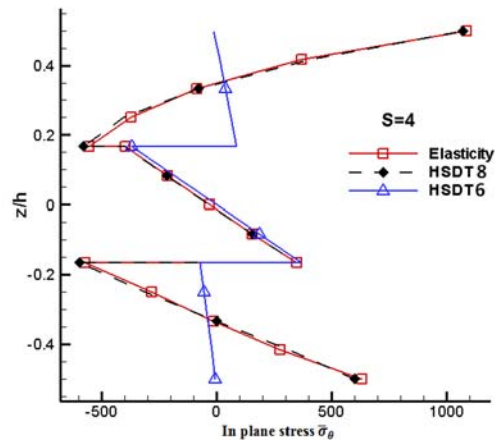**Figure 6**: Varaition of deflection $\overline{w}$ under thermal loading for (90/0/90) shell strip

Figure 7: In-plane stress $\overline{\sigma}_{\theta}$ under thermal for (90/0/90) shell strip

Table 5 compares the results for deflection obtained by HSDT8, HSDT6 (HSDT8 without the higher order terms in w) and CST with results obtained from 3-D elasticity solution. It can be seen that HSDT6 demonstrates a marked accuracy deterioration in the deflection especially at low values of aspect ratio (R/h<10). Thus HSDT6 as well as CST, without the thickness stretching effect being considered, ends up with a very poor estimation of deflection for low values of R/h.
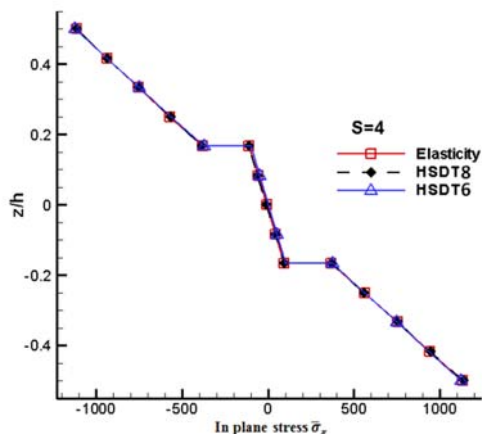
Figure 8: In-plane stress $\bar{\sigma}_x$ under thermal loading for (90/0/90) shell strip
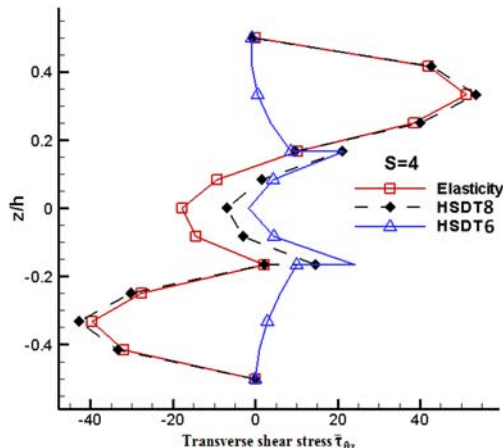

Figure 9: Transverse shear stress $\bar{\tau}_{\theta z}$ under thermal loading for (90/0/90) shell strip

R/h	HSDT8	HSDT6	CST	Elasticity
4	19.80	2.147	3.145	19.754
10	5.869	2.950	3.145	5.860
20	3.830	3.096	3.145	3.827
50	3.257	3.139	3.145	3.255
100	3.175	3.145	3.145	3.171

* z values are given in parentheses; θ values are such that the sin or cos function become a maximum

Table 5: Dimensionless maximum deflection $\bar{w}$(-h/2)* of (90/0/90) shell strip under thermal load

Thus from above Tables 1-5 and Fig 4-9, it is clear that for mechanical/thermal loading, the displacements and stresses obtained using HSDT8 which account for both thickness stretch effect in w and zig-zag function in v agree very well with those obtained by 3D elasticity solution even for thick laminate with R/h = 4.

3.2 Results for Hygrothermal Loading

Having validated the higher order model HSDT8, a study on the effect of combined loading-thermal and hygroscopic load on the bending response of simply supported (90/0/90) laminated cylindrical shell strip is analyzed.

A linear variation of moisture and thermal distribution across the shell thickness is considered.

$$T = 2\overline{T}_0 \left(\frac{z}{h}\right) \sin(m\pi\theta/\theta_m) \quad \text{and} \quad C = 2\overline{C}_0 \left(\frac{z}{h}\right) \sin(m\pi\theta/\theta_m) \tag{22}$$

where $\overline{T}_0$ and $\overline{C}_0$ are the temperature and moisture concentration that are assumed to be $300^{\circ}K$ and 0.01% respectively, where θ_m is taken to be 1 radian and m=1.

Also the thermal and moisture expansion coefficients are assumed to be(Zenkour et al., 2014):

$$\alpha_T = 22.5 * 10^{-6}/^{\circ}K \quad ; \quad \alpha_L = 0.02 * 10^{-6}/^{\circ}K$$
$$\beta_L = 0 \, ; \beta_T = 0.6 \, (\text{wt. } \%H_2O)^{-1}$$

Table 6 shows the results for deflections of (90/0/90) laminated cylindrical shell strip under combined loads (hygrothermal). When comparing with the results from Table 4, one can see that the hygrothermal load affects the deflection and stresses more than the thermal loading and in some cases, it is almost twice the value of thermal case, as reported for laminated plates (Zenkour et al., 2014).

R/h	Theory	$\overline{w}(\pm h/2)^{*}$	$\overline{v}(\pm h/2)$	$\overline{\sigma}_x(\pm h/2)$	$\overline{\sigma}_\theta(\pm h/6)$	$\overline{\tau}_{\theta z}(\pm h/6)$
4	HSDT8	24.75	1.31	-2103.6	-818.70	19.44
		24.94	7.49	2128.6	757.10	11.65
10	HSDT8	8.83	1.23	-2107.6	-803.60	7.12
		8.82	2.99	2121.9	773.84	3.29
20	HSDT8	6.50	1.47	-2110.6	-796.50	3.36
		6.50	2.30	2118.1	781.16	2.95
50	HSDT8	5.84	1.67	-2112.7	-791.97	1.30
		5.84	1.99	2.115.7	785.77	1.23
100	HSDT8	5.76	1.74	-2.113.4	-790.42	0.64
		5.76	1.90	2.114.9	787.32	0.63

* z values are given in parentheses; θ values are such that the sin or cos function become a maximum

Table 6: Dimensionless maximum displacements and stresses of cross–ply (90/0/90) cylindrical shell strips subjected to hygrothermal loading
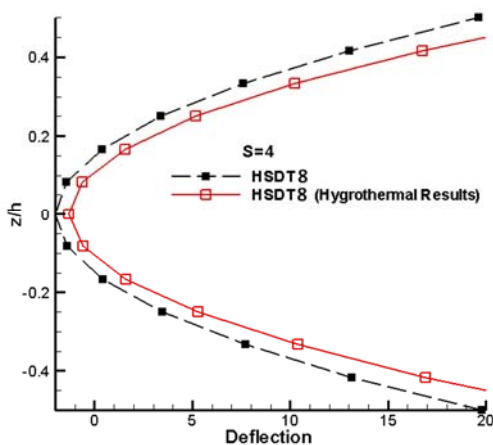

Figure 10: Varaition of deflection $\overline{w}$ under thermal and hygrothermal loading for (90/0/90) shell strip
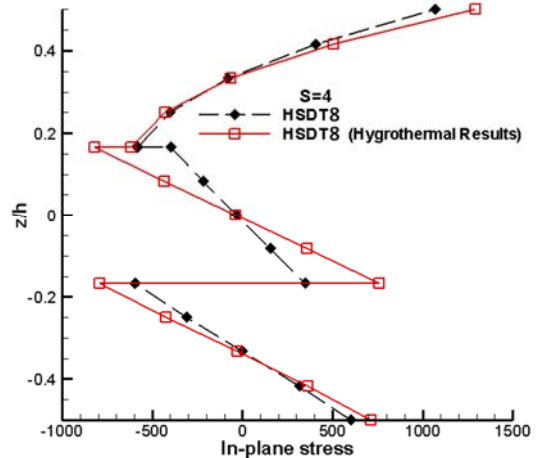
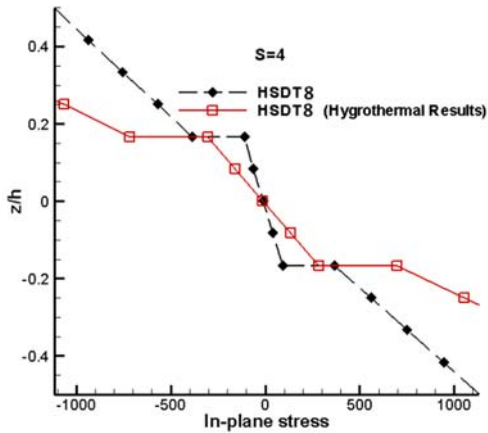**Figure 11**: In-plane stress $\overline{\sigma}_\theta$ under thermal and hygrothermal loading for (90/0/90) shell strip

Figure 12: In-plane stress $\overline{\sigma}_x$ under thermal and hygrothermal loading for (90/0/90) shell strip
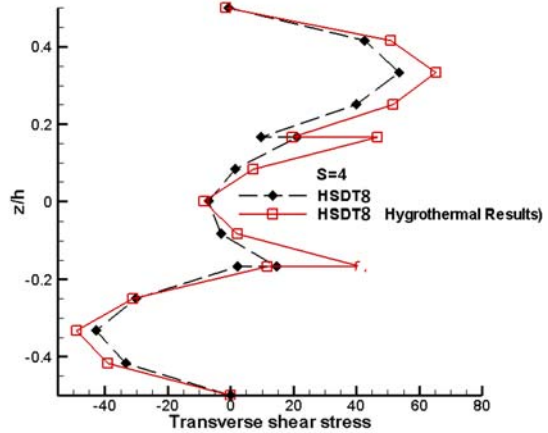
Figure 13: Transverse shear stress $\overline{\tau}_{\theta z}$ under thermal and hygrothermal loading for (90/0/90) shell strip

Fig 10-13 shows the thickness-wise variation for deflections and stresses of a (90/0/90) laminated cylindrical shell strip under both thermal and hygrothermal loading for a very thick laminate(S=4). When comparing the results for hygrothermal loading with the results from thermal loading, one can see that the hygrothermal load affects the deflection and stresses more than the thermal loading and it can be seen that the stresses increases prominently at the interfaces and in some cases it is almost twice the value of thermal case.

4   CONCLUSION

Thermoelastic solutions for orthotropic cylindrical shells under thermal loading have been presented. Useful benchmark results based on elasticity have been presented for cross-ply laminated cylindrical shell strip. A new accurate higher order theory (HSDT8) based on realistic variations of displacements from the elasticity has been proposed. The results of the proposed model were validated against 3D elasticity solution and found to predict well both the stresses and displacements, even for a thick laminate. Numerical results are presented for various cross-ply layup of cylindrical laminated shell strips under thermal loading. The graphical and tabular results presented bring out clearly the importance of higher order terms in the present theory HSDT8. It was found that for thick laminated shells, inclusion of the thickness stretch/contraction effects are more important only for thermal loading whereas the accounting for the interface slope discontinuity (zig-zag function) of the in-plane displacements is essential for both mechanical and thermal loading. It is believed that the results presented here will serve as benchmark in future.

References

Ahmed K. Noor, W.Scott Burton and Peter Geame M. (1991). Assessment of computational models for multilayered composite cylinders. International Journal of Solids and Structures, Volume 27(10), 1269–1286.

Ahmed Noor K and Scott Burton W. (1992). Computational Models for High-Temperature Multilayered Composite Plates and Shells. Appl. Mech., Rev. 45(10), 419-446.

Bhaskar, K., & Varadan, T. K. (1993). Elasticity solution for laminated anisotropic cylindrical shells. Journal of Applied Mechanics, 6(March 1993), 1–7.

Bhaskar, K., Varadan, T. K., & Ali, J. S. M. (1996). Thermoelastic solutions for orthotropic and anisotropic composite laminates. Composite :part B, 8368(96), 415–420.

Brischetto, S. (2013). Hygrothermoelastic analysis of multilayered composite and sandwich shells. Journal of Sandwich Structures and Materials, 15(2), 168–202.

Brischetto, S., & Carrera, E. (2008). Thermal Stress Analysis by Refined Multilayered Composite Shell Theories. Journal of Thermal Stresses, 32(1-2), 165–186.

Brischetto, S., & Carrera, E. (2012). Static analysis of multilayered smart shells subjected to mechanical, thermal and electrical loads. Meccanica, 48(5), 1263–1287.

Huang, NN. and Tauchert TR. (1992). Thermal stresses in doubly-curved cross-ply laminates. International Journal of Solids and Structures, 29(8), 991–1000.

Huang, NN, & Tauchert, TR. (1991). Thermoelastic solution for cross-ply cylindrical panels. Journal of Thermal Stresses, Volume 14(2), 37–41.

Kewei, D. & Limin, T. (1998). Exact Thermoelastic Solution for an Axisymmetric Problem of Thick Closed Laminated Shells. Journal of Thermal Stresses, 21(7), 751–761.

Khare, R. K., Kant, T., & Garg, A. K. (2003). Closed-form thermo-mechanical solutions of higher-order theories of cross-ply laminated shallow shells. Composite Structures, 59(3), 313–340.

Khdier, A. (1996). Thermoeslastic analysis of cross-ply laminated circular cylinderical shells. International Journal of Solids and Structures, 33, 4007–4017.

Lal, A., Singh, B. N., & Anand, S. (2011). Nonlinear bending response of laminated composite spherical shell panel with system randomness subjected to hygro-thermo-mechanical loading. International Journal of Mechanical Sciences, 53(10), 855–866.

Mehrabadi, S. J., & Aragh, B. S. (2013). On the thermal analysis of 2-D temperature-dependent functionally graded open cylindrical shells. Composite Structures, 96, 773–785.

Murakami, H. (1986). Laminated Composite Plate Theory With Improved In-Plane Responses, 53(September 1986), 661–666.

Naidu, N. V. S., & Sinha, P. K. (2005). Nonlinear finite element analysis of laminated composite shells in hygrothermal environments. Composite Structures, 69(4), 387–395.

Nosier, A., & Miri, A. K. (2009). Boundary-layer hygrothermal stresses in laminate composite circular cylindrical shell panels. Archive of Applied Mechanics, 80(4), 413–440.

Pagano, N. J. (1970a). Exact solutions for rectangular bidirectional composites and sandwich plates. Journal of Composite Materials, 4, 20-34.

Pagano, N. J. (1970b). Influence of Shear Coupling in Cylindrical Bending of Anisotropic Laminates. Journal of Composite Materials, 4(3), 330–343.

Pelletier, J. L., & Vel, S. S. (2006). An exact solution for the steady-state thermoelastic response of functionally graded orthotropic cylindrical shells. International Journal of Solids and Structures, 43(5), 1131–1158.

Qatu, M. S. (2012). Review of Recent Literature on Static Analyses of Composite Shells: 2000-2010. Journal of Composite Materials, 02(03), 61–86.

Ren, J. G. (1987). Exact solutions for laminated cylindrical shells in cylindrical bending. Composites Science and Technology, 29(3), 169–187.

Sayman, O. (2005). Analysis of multi-layered composite cylinders under hygrothermal loading. Composites Part A: Applied Science and Manufacturing, 36(7), 923–933.

W. Scott Burton, A. K. N. (1994). Three-dimensional solutions for thermomechanical stresses in sandwich panels and shells. Journal of Engineering Mechanics, Vol. 120, pp. 2044–2071.

Wylie, R. C. and Barrett, L. C. (2012). "Advanced Engineering Mathematics." Tata Mc Graw Hill Education Pvt Ltd, New Delhi.

Xia, L., & Ding, K. (2001). Three-dimensional thermoelastic solution for laminated cantilever cylindrical shell. Aerospace Science and Technology, 5(5), 339–346.

Yifeng, Z., & Yu, W. (2011). A variational asymptotic approach for hygrothermal analysis of composite laminates. Composite Structures, 93(12), 3229–3238.

Zenkour, A. M., Mashat, D. S., & Alghanmi, R. A. (2014). Hygrothermal analysis of antisymmetric cross-ply laminates using a refined plate theory. International Journal of Mechanics and Materials in Design, 10(2), 213–226.